AIRBORNE AND GROUND-BASED INVESTIGATIONS OF THE NORTH FORK OF YELLOW CREEK, JEFFERSON COUNTY, OHIO

Jennifer S. Mabie, Department of Geology and Geography
West Virginia University, Morgantown, WV

Richard W. Hammack and Garret A. Veloski
U.S. Department of Energy, Pittsburgh, PA

Abstract

In the early 1990's, a large inflow of acid mine drainage occurred on the North Fork of Yellow Creek. Underlying coal/clay mines were initially thought to be the source of the contaminated water (a mine "blowout") but historical records showed no mining beneath the impacted area. However, an above-drainage coal mine located about 70 m northeast of the impacted area is a known source of highly acidic water. Although the surface discharge from this mine enters the North Fork of Yellow Creek about 20 m downstream from the impacted area, it is possible that groundwater could flow westward through a narrow area of alluvial deposits to emerge in the streambed at the site of the "blowout". This study used night-time thermal infrared imagery to identify areas where groundwater discharges to the surface (mine discharges, seeps, and springs). The thermal infrared survey identified numerous seeps and springs but no previously unknown mine discharges. A terrain conductivity survey was employed to map a contaminated surface and groundwater plume between the known mine adit and the North Fork of Yellow Creek. This survey showed that the adit was probably not the source of contaminated water at the "blowout" area because both the surface water and groundwater from this mine entered the North Fork of Yellow Creek below the impacted area. The survey did not identify the actual source of contaminated water at the "blowout". Results of this study indicated that the concrete seal installed in the North Fork of Yellow Creek to prevent large inflows of acid mine drainage was effective.

Introduction

On May 17, 1991, a sudden influx of acid mine drainage (AMD) resulted in a major fish kill in the North Fork of Yellow Creek near Hammondsville in Jefferson County, Ohio (Fig. 1). Initially, the source of the AMD was thought to be a blowout from a flooded mine (Fig. 2) in a coal/clay bed (lower coalbed, Fig. 3) that occurs about 20 ft beneath the stream. Based on this assumption, the Ohio Division of Natural Resources constructed a concrete seal at the site of the "blowout" that was intended to prevent or curtail the flow of AMD into the stream. Though the seal, completed in June 1993, has been successful in preventing large influxes of AMD into the stream, AMD continues to seep into the streambed at the location of the seal.

Since the seal emplacement, a review of historical records has indicated that no known mining occurred at the location of the “blowout”. The closest known source of AMD is an above-drainage drift mine (Fig. 2) located in the upper coalbed (Fig. 3). Highly contaminated water from this mine discharges into a wetland area within a cut-off meander of the North Fork of Yellow Creek. The AMD then flows slowly southward through a series of shallow pools until it enters the North Fork of Yellow Creek (Fig. 2), about 20-m downstream from the suspected mine “blowout”.

This study focuses on the Hammondsville Reclamation Site, located in Jefferson County, Ohio (Fig. 1) approximately 2.5 miles southwest of the Ohio River. Airborne thermal infrared (TIR) imaging and ground-based electromagnetic (EM) methods were used to evaluate the effectiveness of the concrete seal and to determine the source(s) of AMD entering the stream in the vicinity of the blowout. The U.S. Department of Energy, National Energy Technology Laboratory (NETL) conducted the investigation with funding provided by the U.S. Army Corp. of Engineers.

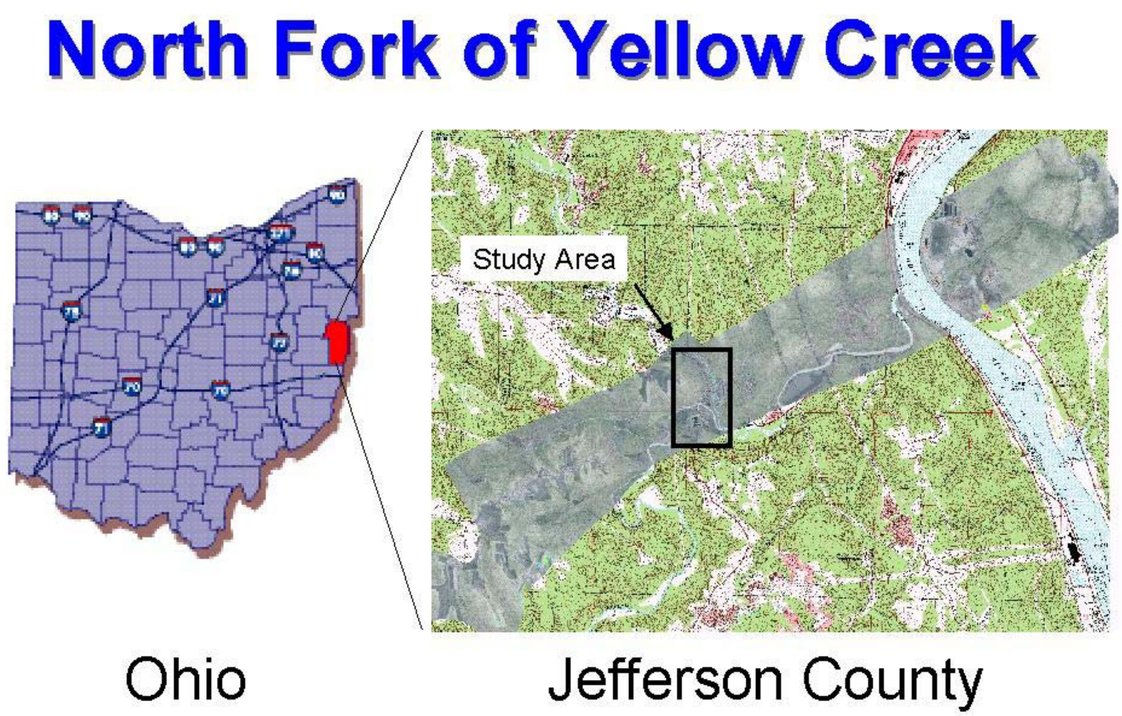

Figure 1. Location of Hammondsville Remediation Site.

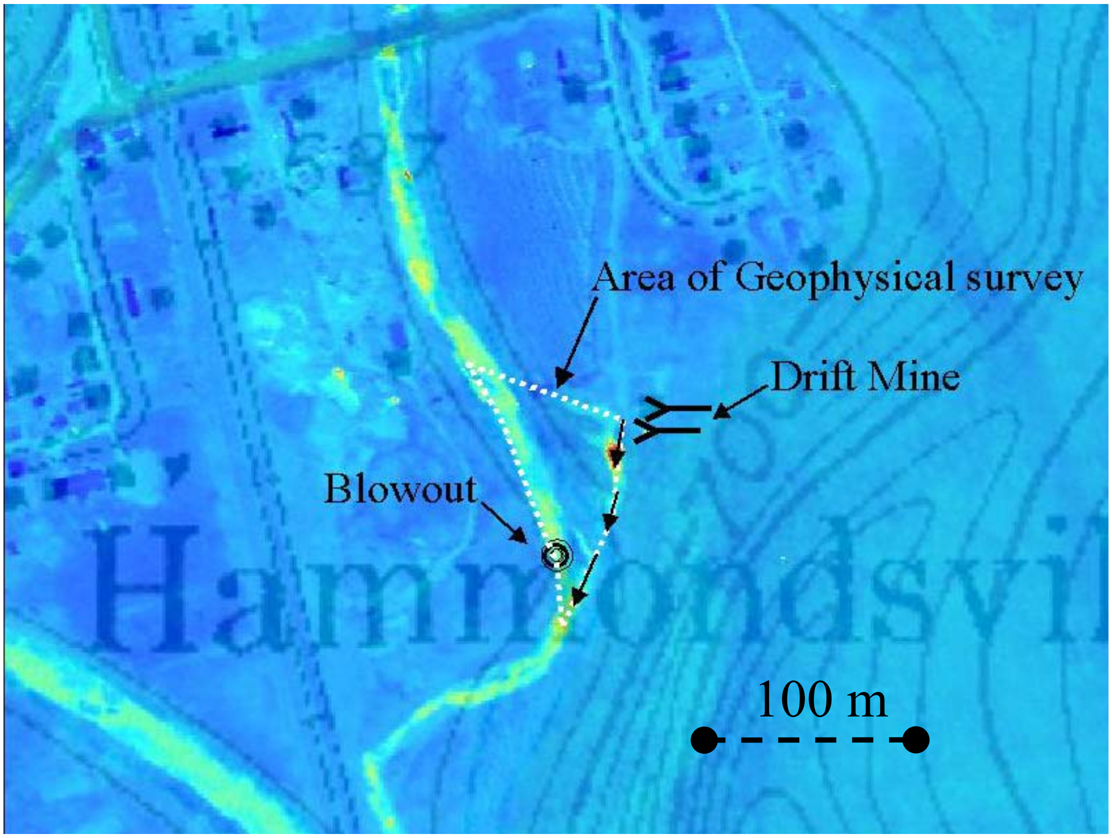

Figure 2. AMD from the drift mine discharges to an area of wetlands and shallow pools, and eventually enters the North Fork of Yellow Creek about 20 meters downstream of the blowout area.

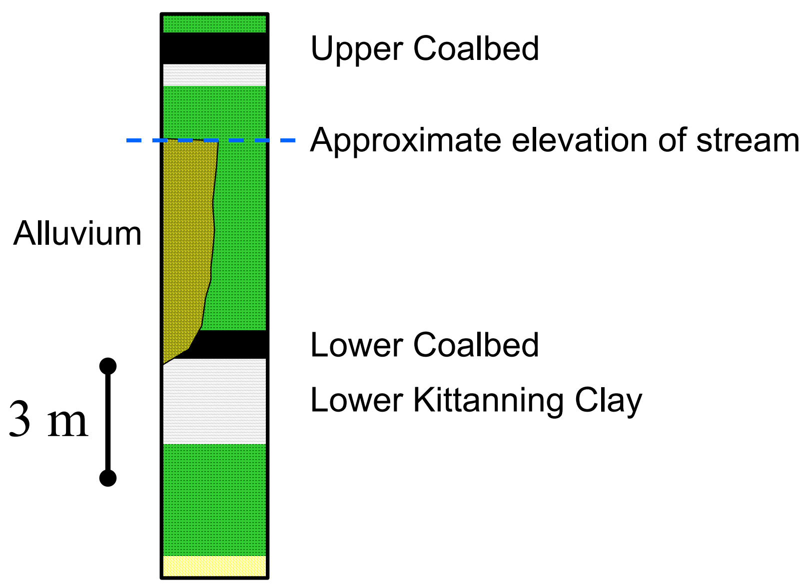

Figure 3. Generalized geologic section.

Methods

Airborne Thermal Infrared Survey

Airborne thermal infrared images were obtained for the project area as part of a 27-km^2 survey of the lower reaches of Yellow Creek (Figs. 1 and 2). The thermal imagery was acquired from a Piper Aztec platform using a SynSyTech 11-channel, multispectral line scanner (MLS). The MLS was configured for nighttime thermal operation with a spectral sensitivity range of 8.5-12.5µm (band 1) in the far infrared. A position and orientation system (POS) was used to correct images for distortions brought about by aircraft attitude (Brewster, 1999). The thermal and spatial resolution for this survey was 0.1ºC and 1-meter, respectively.

Thermal data was acquired between 3:00 am and 6:00 am in the winter months (a leaf-off period) to ensure optimal thermal contrast between cold surface water and warmer ground water from mine discharges, seeps, and springs. This time window allows objects heated by sunlight during the day to reach temperature equilibrium with the surroundings and minimizes the effects of radiation emitted by the atmosphere. Water has a high thermal inertia, or a high retention of thermal energy due to high specific heat; whereas land features have a lower retention of heat. This contrast makes nighttime data acquisition well suited for this investigation. The spectral radiant emittances for most surface features are optimal in the far infrared band (8-14um) (Lillesand and Keifer, 1994). Thresholding, the application of color look-up tables, and density slicing allowed for the water features to be easily distinguished (Richards, 1994).

Terrain Conductivity Surveys

Conductivity varies within the earth and is controlled by the rocks and soil that make up the subsurface. Factors that influence ground conductivity are: porosity, moisture content, dissolved electrolyte content, temperature and phase state of pore water, and the amount and composition of colloids (McNeill, 1980a).

The EM-31 and EM34-3XL use an artificially generated alternating electromagnetic field to probe the earth's subsurface for conductivity variations. Passing an alternating current of fixed frequency through a transmitter coil produces a dipole primary magnetic field of constantly varying intensity. The primary field penetrates into the earth and induces the flow of current in conductors in the ground. The ground currents, in turn, generate a secondary field that is phase shifted 90° - 180° from the primary field. The receiver coil of the instrument senses the secondary magnetic field produced by ground currents.

The strength of the secondary field is dependent on the spacing of the transmitter and receiver coil, the frequency of the primary field, and the ground conductivity. McNeill (1980b) describes a simple linear relationship that relates the ratio of the secondary and primary fields to the apparent conductivity of the ground.

$$\frac{H_s}{H_p} = \frac{i\omega\mu_0\sigma s^2}{4}$$

Where:

H_s is the secondary magnetic field at the receiver coil
H_p is the primary magnetic field at the receiver coil
ω is equal to $2\pi f$
f is the frequency of alternating current in transmitter coil
μ_0 is permeability of free space
σ is ground conductivity
s is the intercoil spacing
i is square root of -1.

A terrain conductivity instrument directly measures the primary and secondary magnetic fields. Therefore, the H_s/H_p ratio is known and the apparent conductivity can be calculated.

The effective exploration depth for terrain conductivity surveys is assumed to be one half of the skin depth. The skin depth is the depth at which the amplitude of the electromagnetic field drops to 1/e of the source amplitude, e being the natural base, and is a function of the operating frequency (f) and the ground conductivity (σ). The skin depth (δ) is given by the following relationship:

$$\delta = 503(1/\sigma f)^{1/2}$$

The skin depth is inversely proportional to the frequency of the electromagnetic wave. Therefore, to obtain a greater exploration depth, a lower frequency should be used.

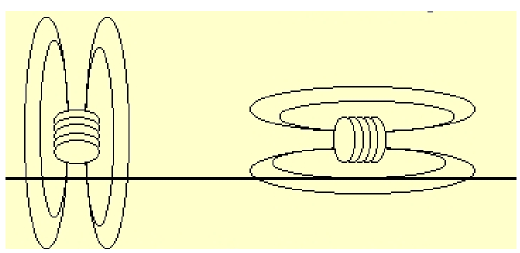

Figure 5. Magnetic field vectors around a transmitter coil with a vertical dipole orientation (left) and a horizontal dipole orientation (right).

The effective exploration depth increases with increased intercoil spacing. The exploration depth also depends on coil orientation. Generally, the effective depth of exploration is greater when the instrument operates with the transmitter and receiver coils in the vertical dipole orientation (Fig. 5). Combined use of the EM31 and the EM34-3XL instruments can provide observations at four different intercoil spacings and two different coil orientations. The coil spacing for the EM31 is fixed at 3.67 meters, which has an effective exploration depth of 2.75 meters in the horizontal dipole orientation and 5.5 meters in the vertical dipole orientation. The EM34-3XL has three different coil spacings: 10 meters, 20 meters, and 40 meters. The effective exploration depth in the horizontal dipole field is 7.5 m, 15 m, and 30 m, respectively; the effective exploration depth in the vertical dipole field is 15 m, 30 m, and 60 m, respectively. For this survey, the 10-m coil spacing was used.

Geonics EM-31 and EM34-3XL electromagnetic conductivity instruments were used to measure terrain conductivity along three sub-parallel traverses. The three lines are depicted in Figure 7 with ‘+’ symbols. Line 1 is a segment of a 620-m traverse along the North Fork of Yellow Creek between State Route 213 bridge and a railroad bridge downstream from the “blowout” area. Line 2 is a 100-m traverse along a game trail adjacent to the North Fork of Yellow Creek. Line 3 is a 100-m traverse along the flowpath taken by AMD from the mine adit to the North Fork of Yellow Creek.

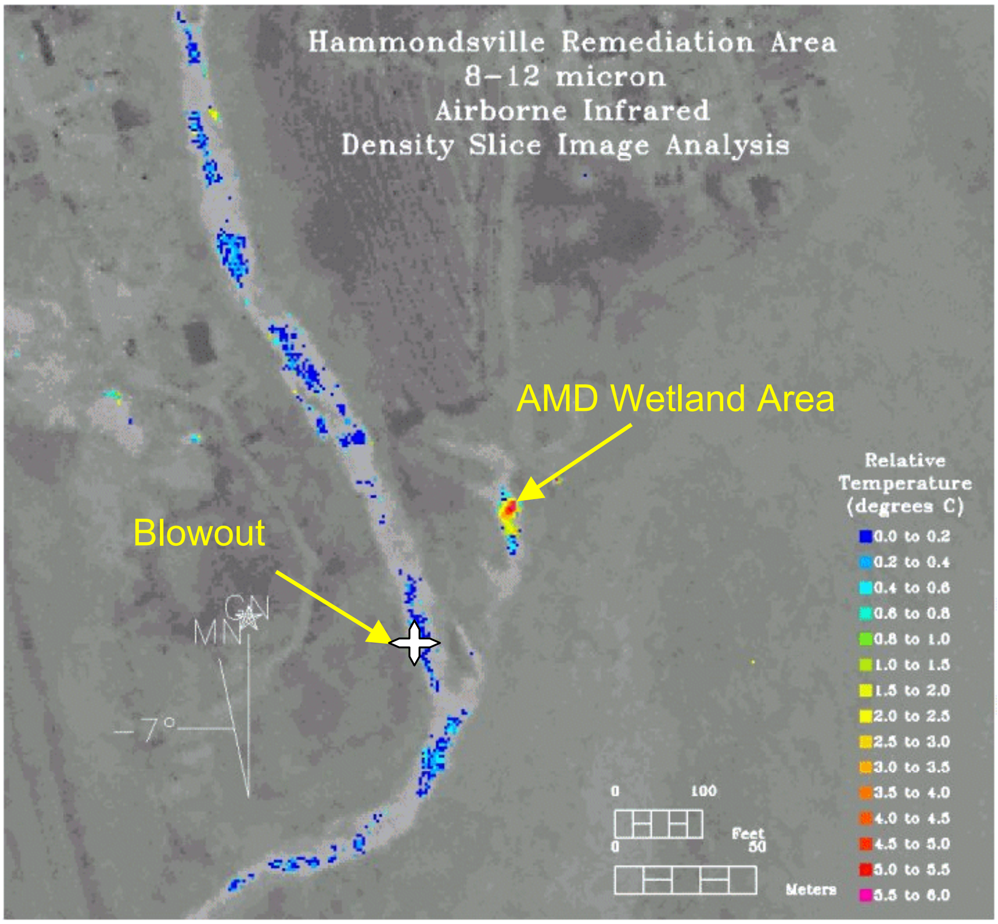

Figure 6. Density slice image analysis of TIR data in vicinity of study area. Color scale indicates apparent temperatures of water features.

Results and Discussion

Thermal Infrared Imagery

A density slice of the thermal infrared image of the project area is displayed in Figure 6. Two thermal anomalies were identified: the drift mine discharge into a wetland area, and an anomaly that is presumed to be a sewage or gray water discharge. No thermal anomalies were observed in the vicinity of the blowout area.

Geophysical Surveys

Apparent conductivity maps of the project area were obtained using an EM31 (Figure 7A) and an EM34-3XL with 10-m coil spacing (Figure 7B).

Conductivity values in Figure 7A were obtained with an EM31 using a horizontal and vertical dipole coil orientation. Conductive anomalies along the eastern boundary of the surveyed area coincide with the location of shallow pools of acidic, metal-containing mine drainage, which form the wetland area. Resistive ground separates the conductive anomalies in the east from the North Fork of Yellow Creek along the western survey boundary. The North Fork of Yellow Creek only intercepts the conductive anomaly where the surface flow from the mine enters the North Fork of Yellow Creek. Combining the horizontal and vertical dipole orientations provides a useful vertical image of ground conductivity to a depth of 5.5m (18 ft). These surveys suggest that there is no shallow (<5.5-m depth) flow of contaminated groundwater between the AMD-impacted wetland at the above-drainage mine adit and the North Fork of Yellow Creek at the location of the "blowout."

Conductivity maps were also acquired using an EM34 (10-m coil spacing) with horizontal and vertical dipole coil orientation (Figure 7B). Like the conductivity maps acquired using the EM31, these maps indicated the existence of a conductivity anomaly along the eastern boundary of the surveyed area at the AMD-impacted wetland location. The EM34 with a vertical dipole orientation and a 10-m intercoil spacing has the greatest exploration depth (15 m or 50 ft) but is insensitive to the conductivity of near-surface materials. Using this configuration, the EM34 measures the conductivity of strata at or below the depth of the lower coalbed but ignores near-surface conductors such as AMD in pools and wetland areas. As expected, the conductivity at depth is much less than at the surface. However, a conductivity anomaly was identified at depth beneath the AMD source, which suggests that AMD is not completely contained at the surface, but may be infiltrating into underlying strata. The conductive anomaly at the AMD source is separated from a second conductive anomaly at the site of the blowout by area of slightly more resistive ground. The conductive anomaly at the AMD source is not connected with the anomaly at the blowout within the surveyed area.

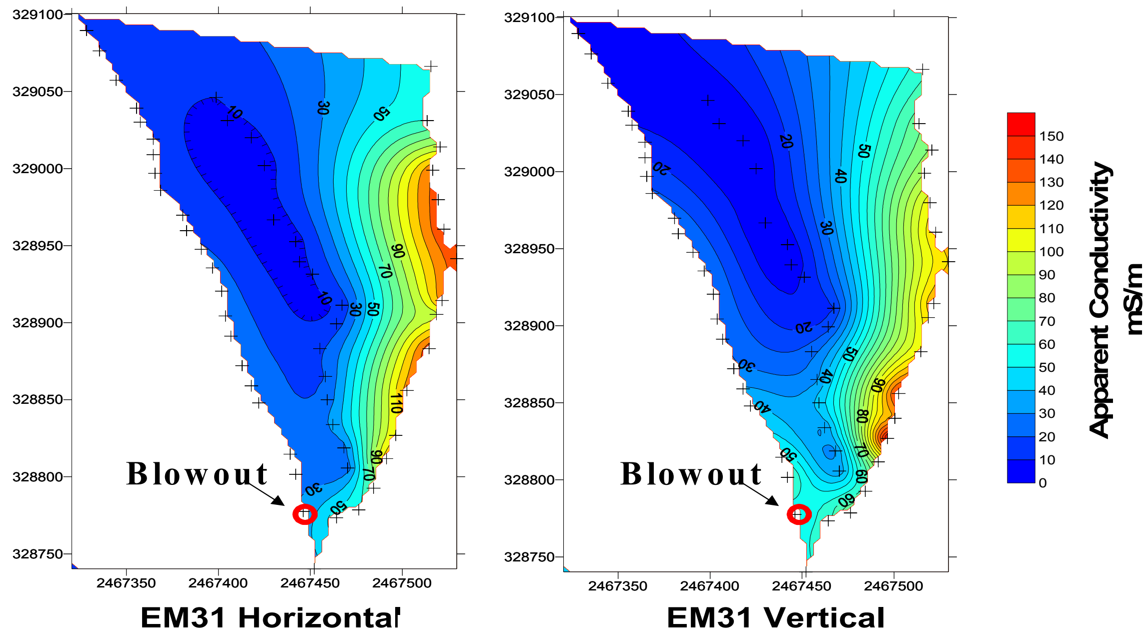

Figure 7A

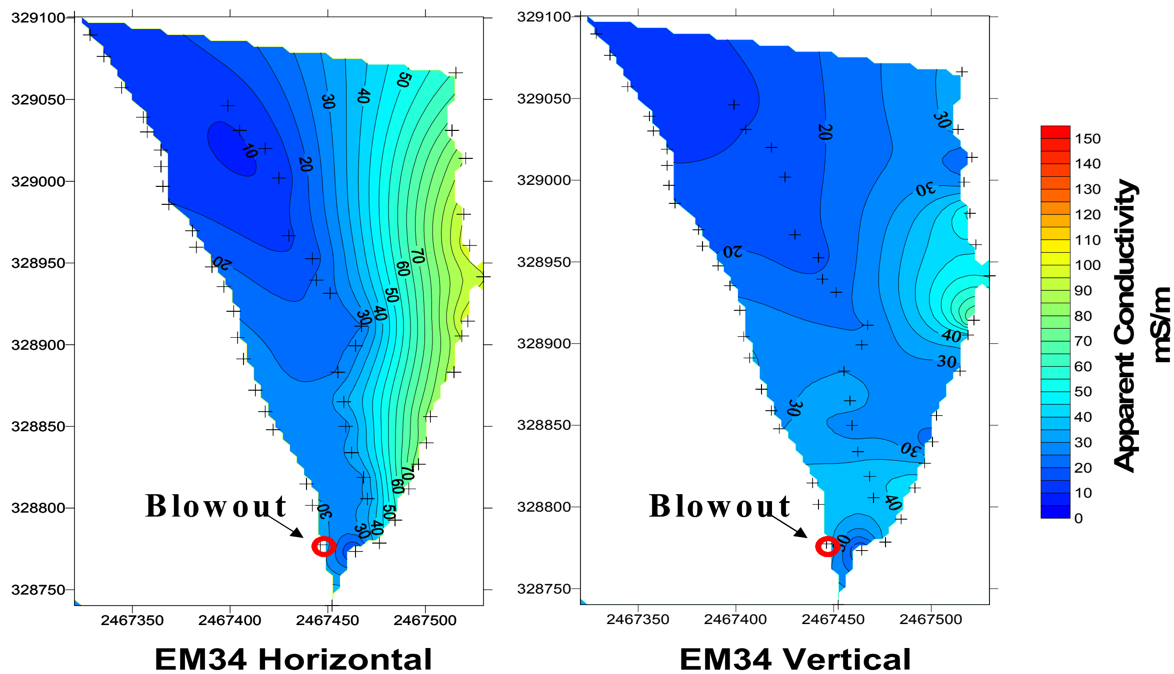

Figure 7B

Figure 7. Conductivity maps of Hammondsville Remediation Site. A: EM31 survey; B: EM34 survey. Note that grid coordinates are in U.S. feet, Ohio State Plane North.

Conclusions

No thermal infrared anomalies or near-surface conductivity anomalies were observed in the North Fork of Yellow Creek in the vicinity of the "blowout" area. This suggests that the seal is effectively preventing acid mine drainage from entering the stream from a source below the stream.

EM31 and EM34 surveys suggest that AMD does not flow from the drift mine to the "blowout" site via near-surface alluvial aquifers. Rather, AMD flow to the "blowout" site may occur via a confined aquifer in the lower coal bed. It is unlikely that the discharge from the drift mine could be the sole source of the high volume of contaminated water discharged at the "blowout" site. Therefore, other mines in the area may be implicated as potential sources of the AMD in the lower coalbed aquifer.

Acknowledgements

The authors wish to acknowledge the U.S. Army Corps of Engineers, Pittsburgh District for funding this project and providing background data. Thanks are also extended to Jim Gue of the Ohio Department of Natural Resources for providing information about the construction of the concrete seal at the site of the "blowout".

References

Michael Baker, Jr., Inc. 2001. North Fork Yellow Creek, Hammondsville, Ohio, Section 206 Aquatic Ecosystem Restoration, Preliminary Design and Alternatives Formulation Meeting, June 7, 2001.

Brewster, S. B. 1999. Geometric Correction System Capabilities, Processing, and Applications. Proceedings of the Fourth International Airborne Remote Sensing Conference and Exhibition/21st Canadian Symposium on Remote Sensing. June 21-24, 1999, Ottawa, Ontario, Canada.

Gue, Jim, Ohio Department of Natural Resources, personal communication January 16, 2002.

Lillesand, T. M. and R. W. Kiefer. 1994, Remote Sensing and Image Interpretation, 3rd Ed. John Wiley & Sons, Inc., New York, NY

McNeill, J. D., 1980a. Electrical Conductivity of Soil and Rocks, TN-5. Geonics Limited. Ontario, Canada. 22p.

McNeill, J.D. 1980b. Electromagnetic Terrain Conductivity Measurement at Low Induction Number, TN-6. Geonics Limited. Ontario, Canada. 15 p.

Richards, J. A. 1994. Remote Sensing Digital Image Analysis. Springer-Verlag, Berlin, German Republic, 340p.